Percutaneous contrast echocardiography-guided intramyocardial injection and cell delivery in a large preclinical model

Article

Accepted Version

TITLE:
Percutaneous Contrast Echocardiography-guided Intramyocardial Injection and Cell Delivery in a Large Preclinical Model

AUTHORS & AFFILIATIONS:
Alejandro Giraldo[1]*, Jesús Talavera[2]*, María Josefa Fernández-del-Palacio[2], Obdulio García-Nicolás[3,4], Juan Seva[4], Gavin Brooks[1], José María Moraleda[5]

[1]Institute for Cardiovascular and Metabolic Research, School of Biological Sciences, University of Reading, Reading, United Kingdom
[2]Departamento de Medicina y Cirugía Animal, Facultad de Veterinaria, Universidad de Murcia, Murcia, Spain
[3]Institute of Virology and Immunology (IVI), Mittelhäusern, Switzerland (Present address)
[4]Departamento de Anatomía y Anatomía Comparada, Facultad de Veterinaria, Universidad de Murcia, Murcia, Spain
[5]Unidad de Trasplante Hematopoyético y Terapia Celular, Departamento de Hematología, Hospital Universitario Virgen de la Arrixaca, IMIB, Universidad de Murcia, Murcia, Spain
*These authors contributed equally

EMAIL ADDRESSES:
Alejandro Giraldo (a.giraldoramirez@reading.ac.uk)
Jesús Talavera (talavera@um.es)
María Josefa Fernández-del-Palacio (mjfp@um.es)
Obdulio García-Nicolás (obdulio.garcia-nicolas@ivi.admin.ch)
Juan Seva (jseva@um.es)
Gavin Brooks (g.brooks@reading.ac.uk)
José María Moraleda (jmoraled@um.es)

CORRESPONDING AUTHORS:
Alejandro Giraldo (a.giraldoramirez@reading.ac.uk)
Jesús Talavera (talavera@um.es)

KEYWORDS:
Animal model, cardiomyopathy, cell therapy, contrast echocardiography, intramyocardial injection, heart failure.

SHORT ABSTRACT:
Novel therapeutic strategies in cardiac regenerative medicine require extensive and detailed studies in large preclinical animal models before they can be considered for use in humans. Here, we demonstrate a percutaneous contrast echocardiography-guided intramyocardial injection technique in rabbits, which is valuable for hypothesis testing the efficacy of such novel therapies.

LONG ABSTRACT:
Cell and gene therapy are exciting and promising strategies for the purpose of cardiac regeneration in the setting of heart failure with reduced ejection fraction (HFrEF). Before they can be considered for use, and implemented in humans, extensive preclinical studies

are required in large animal models to evaluate the safety, efficacy, and fate of the injectate (*e.g.*, stem cells) once delivered into the myocardium. Small rodent models offer advantages (*e.g.*, cost effectiveness, amenability for genetic manipulation); however, given inherent limitations of these models, the findings in these rarely translate into the clinic. Conversely, large animal models such as rabbits, have advantages (*e.g.*, similar cardiac electrophysiology compared to humans and other large animals), whilst retaining a good cost-effective balance. Here, we demonstrate how to perform a percutaneous contrast echocardiography-guided intramyocardial injection (IMI) technique, which is minimally invasive, safe, well tolerated, and very effective in the targeted delivery of injectates, including cells, into several locations within the myocardium of a rabbit model. For the implementation of this technique, we also have taken advantage of a widely available clinical echocardiography system. After putting in practice the protocol described here, a researcher with basic ultrasound knowledge will become competent in the performance of this versatile and minimally invasive technique for routine use in experiments, aimed at hypothesis testing of the capabilities of cardiac regenerative therapeutics in the rabbit model. Once competency is achieved, the whole procedure can be performed within 25 min after anaesthetizing the rabbit.

INTRODUCTION:

Cell and gene therapies are exciting and ever developing strategies for regenerating/repairing the injured myocardium in HFrEF. A few studies have compared the effectiveness (*e.g.*, cell retention rate) of the different routes of cell delivery, which have consistently demonstrated the superiority of IMI over intracoronary or intravenous routes[1-5]. Thus, it is not surprising that a large proportion of studies on translational models of stem cell therapy of the injured myocardium, deliver the injectate via IMI performed under direct view in an open chest procedure[6,7]. However, this approach has several limitations, including the invasive nature of the procedure, which carries the risk of peri-procedural mortality (often under-reported)[8]. In addition, an IMI under direct view does not eliminate the possibility for inadvertent injection into the ventricular cavity. In clinical practice an IMI during open chest surgery could be an appropriate method for therapeutic cell delivery, *e.g.*, during coronary artery bypass graft surgery (CABG); however, this approach may not be appropriate for cell delivery in global cardiomyopathy of non-ischemic origin (*e.g.*, HFrEF secondary to anthracycline-induced cardiomyopathy (AICM)).

There is no doubt that ischemic heart disease (IHD) is the most common cause of HFrEF (~ 66%)[9,10]; however, non-ischemic cardiomyopathy, including AICM, still affects a significant proportion of patients with HFrEF (33%)[9]. Indeed, recent advances in clinical oncology have resulted in more than 10 million survivors of cancer in the USA alone[11], with estimates of a similar number in Europe, consistent with an overall trend towards improved survival of cancer patients[12,13]. Thus, exploring the benefits of novel therapies such as stem cell transplant for non-ischemic cardiomyopathy, as well as the trialing of an effective and minimally invasive route of stem cell delivery is of utmost importance, given the increasing number of patients affected by cardiotoxicity secondary to anticancer drugs.

Of note, hypothesis testing studies using stem cell therapy aiming to repair/regenerate the injured myocardium frequently involves the use of small rodents (*e.g.*, mice and rats). These models often require expensive high frequency ultrasound systems for evaluation of

myocardial function, usually equipped with linear array transducers which have some inherent associated limitations (*e.g.*, reverberation)[14]. However, other models such as rabbits, representing a large preclinical model, have some advantages for hypothesis testing of stem cell therapies in HFrEF. Thus, in contrast to rats and mice, rabbits maintain a Ca^{+2} transport system and cellular electrophysiology that resembles that of humans and other large animals (*e.g.*, dogs and pigs)[15-19]. Another advantage, is their amenability for cardiac ultrasound imaging using relatively inexpensive and widely available clinical echocardiography systems equipped with relatively high frequency phase array transducers, *e.g.*, 12 MHz, such as those frequently used in neonatal and pediatric cardiology. These systems allow excellent echocardiographic imaging with state of the art technology, and they take advantage of the superiority of harmonic imaging[20]. Furthermore, extensive hypothesis testing of the potential of cardiac regenerative therapies (*e.g.*, stem cell therapy), their safety, efficacy, cardiomyogenic potential, as well as evaluation of the fate of the injectate once delivered into the myocardium, is mandatory before they can be considered for human use, and they require the use of large preclinical animal models, such as the rabbit[17,19]. Here, we describe a minimally invasive technique for cell delivery via percutaneous contrast-echocardiography guided IMI using a clinical echocardiography system, which is aimed at stem cell transplant-based therapy for non-ischemic cardiomyopathy[20]. We also describe the benefits of India Ink (InI, also known as China Ink) as an ultrasound contrast agent and *in situ* tracer of the injectate in the rabbit heart.

PROTOCOL:

The experiments described herein were approved by the Ethical Research Committee of the University of Murcia, Spain, and were performed in accordance with Directive 2010/63/EU of the European Commission. The steps described were performed under standard operating protocols that were part of the plan of work and have not been performed solely for the purpose of filming the accompanying video to this paper.

1. Preparation of Cells and Mammalian Expression Vector

Note: Here, we briefly describe a protocol for preparation and transfection of a cell line (human embryonic kidney 293 (HEK-293)); however, appropriate cell specific protocols for the cell type of interest should be optimized (*e.g.*, stem cells).

1.1. Maintain HEK-293 cells in high glucose Dulbecco's modified Eagle's medium (DMEM) supplemented with 10% fetal calf serum (FCS), 1% sodium pyruvate, 2 mM Glutamine, 1% penicillin/streptomycin, and incubated at 37 °C in a humidified atmosphere containing 5% CO_2. Once cells are sub-confluent, split at a ratio of 1:3.

1.2. Start splitting the cells by aspirating the media, then wash once with sterile phosphate buffered saline (PBS), remove excess PBS and then incubate with 2.5 mL of 0.5x Trypsin-Ethylenediaminetetraacetic acid (EDTA) (5 min, 37 °C).

1.2.1. Add one volume of DMEM media (supplemented as described above) to stop the reaction, and then detach the cells by slowly and gently aspirating up and down with an electronic pipette.

1.3. Then, transfer the cell suspension to an appropriate container (*e.g.*, 15–50 mL conical centrifuge tube). Centrifuge in a swing bucket (100 x *g*), discard the supernatant and wash the pellet twice with sterile PBS.

1.4. Resuspend the pellet in fresh DMEM media and seed at an appropriate cell density (*e.g.*, 1 x 10^6 cells in a 75 cm^2 flask) in fresh culture flasks or large dishes according to local laboratory practices.

1.4.1. Replace existing media with fresh media every 2 days.

Note: The expression vector was derived from pIRES1hyg and used according to the manufacturer's instructions as previously described[21]. p(EGFP) IRES1hyg was generated by subcloning EGFP cDNA as a BamHI + NotI insert from pEGFP-N1 into the BamHI + NotI digested pIRES1hyg[21].

1.5. 1 day before transfection, seed HEK-293 cells at a density of 0.5 x 10^5 cells/cm^2 in 12- or 24-well tissue culture plates.

1.6. On the day of transfection, prepare DNA-lipid transfection reagent complexes in separate 1.5 mL microcentrifuge tubes (1 tube/well).

1.6.1. Start by adding 250 µL of reduced serum medium into each tube, and then add 4 µg DNA (mix gently).

1.6.2. Subsequently, add 250 µL from a previously prepared mix of 10 µL lipid transfection reagent and 250 µL of reduced serum medium, to each tube (mix again gently).

1.6.3. Finally, proceed with transfections, by incubating HEK-293 cells with DNA lipid transfection reagent complexes for 4 h, and then replace with DMEM medium supplemented as described above (step 1.1), and incubate for another 48 h. Perform drug selection of stable transfectants with 100 µg/mL hygromycin B.

1.7. Detach HEK-293 cells with trypsin as described above (step 1.2). After washing the cells in sterile PBS, resuspend in an appropriate vehicle (*e.g.*, 10% v/v InI in PBS), to achieve a final cell concentration of 5 x 10^6/mL.

2. Preparation of the Rabbit

Note: The positioning of the rabbit and the transducer for IMI is not optimal to evaluate morphology and function of the heart of the animal. Thus, it is advisable to perform a complete echocardiographic examination[20] prior to the IMI (see below), and at subsequent time points as defined by the experimental design. This will aim to evaluate the baseline anatomical and functional characteristics of the heart in the animal that will receive an injection, and also evaluate the effects, of IMI in the function of the heart.

2.1. Perform this examination in a blinded fashion and following the guidelines of the Echocardiography Committee of the American College of Veterinary Internal Medicine and the American Society of Echocardiography/European Association for Cardiovascular Imaging[22-24].

2.2. Obtain a simultaneous 1-lead electrocardiogram (ECG) tracing throughout the whole echocardiographic study.

2.3. Anesthetize the rabbit with ketamine 10 mg/kg, combined with medetomidine 200 µg/kg, intramuscular (I.M.) injection.

2.4. Verify the level of anesthesia after 10–20 min following administration of anesthesia.

2.5. Using a hair clipper remove the hair of the chest widely (*e.g.*, below the neck to the sub-xiphoid region) (**Figure 1A**).

2.6. Shave additional regions of 1–2 cm^2 in the internal face of the right forelimb (mediocubital region) and of both hind limbs (mediotibial region) (**Figure 1B**).

2.7. Place adhesive ECG electrodes on the shaved regions of the limbs to synchronously monitor the heart rhythm during the procedure (**Figure 1C**).

2.8. Place the animal in the decubitus supine position on a thermal blanket, with the limbs outstretched using surgical tape attached to the table (**Figure 1C**).

2.8.1. Make sure the ears are flexed backwards behind the head/back of the rabbit, and at a position that is lower than its forelimbs, since this helps to maintain correct positioning of the thorax of the animal throughout the procedure.

2.9. Allow the animal to breathe spontaneously whilst administering oxygen by face mask throughout the whole procedure (100%, 2–3 L/min).

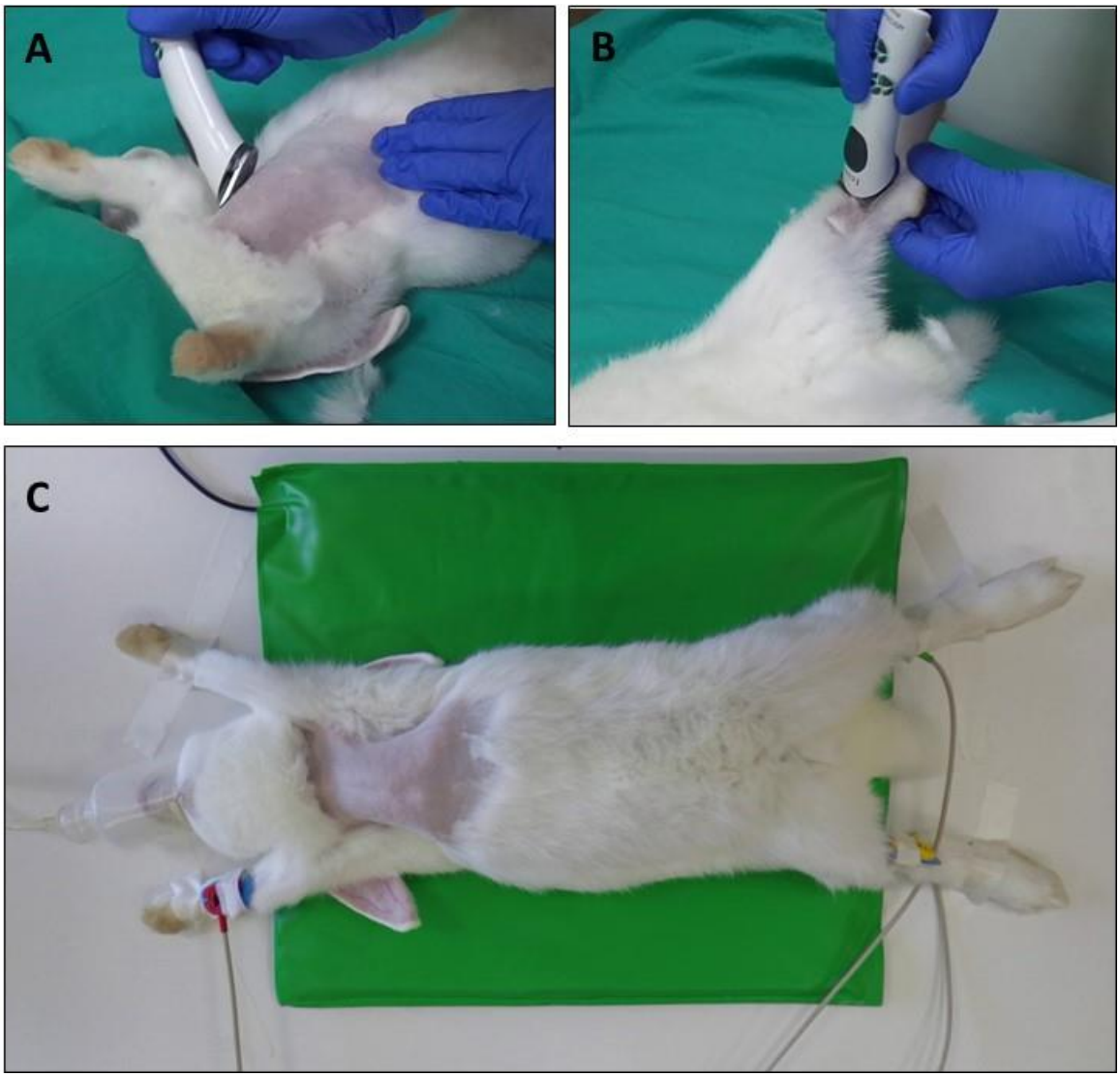

Figure 1. Preparation of the rabbit for IMI. (**A**) Clip hair from thorax; (**B**) Clip hair from limbs; (**C**) Attach electrodes and position the rabbit with legs outstretched on a thermal blanket.

3. Percutaneous Contrast Echocardiography-guided IMI Technique in the Rabbit

3.1. Clean and disinfect the skin of the thorax with a chlorhexidine-based solution.

3.1.1. Use an aseptic technique throughout the whole procedure, according to current best practice.

3.1.2. Whenever possible, and if reasonably practicable, perform a fully sterile procedure, including, but not limited to, the use of sterile material such as gowns, gloves, surgical wound drapes, sterile dressing material for the table, as well as a sterile ultrasound transducer cover and sterile ultrasound gel. This will reduce to a minimum the risk of introducing pathogens to the animal receiving IMI, and is standard practice in the clinical setting (*e.g.*, during cardiac puncture).

Note: It is recommended to always proceed in line with local and national regulations of animal research applicable to the local institution and country of practice.

3.2. Apply ultrasound transmission gel to the chest and/or to the transducer, and with the transducer cord around the experimenter's neck, perform a quick window scan of the animal's heart, which is often helpful to visualize anatomy and to plan for the IMI.

3.3. Place the transducer manually at the 4^{th}–6^{th} intercostal space, 2–3 cm away from the right parasternal line with an angle of incidence of ~ 90° with respect to the right side of the thoracic wall (**Figure 2A**).

3.4. Adjust the location of the transducer relative to the intercostal space as well as its anteroposterior and dorsoventral angle to optimize a modified short axis view at the level of the papillary muscles. Identify in this view the right ventricle (RV), left ventricle (LV), interventricular septum (IVS), posterior wall (PW), as well as anterolateral (AL) and posteromedial (PM) papillary muscles (**Figure 2B**).

3.4.1. Have a wide field of view by significantly increasing the depth using the appropriate control on the system (*e.g.*, button, dial).

3.4.2. Pay particular attention to obtaining a symmetrical image in this view, as well as appropriate differentiation of endocardial and epicardial contours, and, if necessary, adjust through image optimization controls (*e.g.*, gain).

3.5. Once the optimal echocardiographic view is obtained (**Figure 2B**), maintain this position throughout the rest of the procedure, whilst a second operator performs the IMI (see below).

3.5.1. Whilst holding the transducer, avoid concealing the transducer orientation mark, which should always be facing forward, thus allowing its alignment with the needle in subsequent steps (**Figure 2A, C**).

3.6. With a 24-G needle attached to a 1 mL syringe, place the needle close to the skin of the left hemithorax in a symmetric mirroring position with respect to the transducer. Then, manually align the needle with the transducer orientation mark at an angle of ~ 90° (**Figure 2C**), and slowly advance the needle through the skin and into the chest cavity.

Note: The percutaneous needle insertion in this position and orientation facilitates the visualization of the needle in the plane of the ultrasound beam (**Figure 2D, E**), thus allowing real time monitoring and, when necessary, adjustment of the location of the needle relative to the target region of the myocardium (**Figure 2G, H**).

3.7. With the tip at the target location, slowly deliver the injectate (up to 0.25 mL per injection site) within 10–30 s (**Figure 2E**), whilst slowly and gently retracting the needle during injection to increase the extent of the myocardium treated.

3.7.1. Use InI 10% (v/v) diluted in PBS for standardization of the technique, and as an *in situ* tracer whilst acquiring competency, as well as to confirm successful targeting of all four IMI sites within the myocardium by gross pathology and histopathology (see **Representative Results**). Once competency is achieved, InI could be substituted by a suitable commercial ultrasound contrast agent if desired.

Note: Delivery of 10% (v/v) InI diluted in PBS either with or without cells into the myocardium results in transmural hyperechogenicity (*i.e.*, echo bright appearance) at the target site of injection (**Figure 2E, F**). Transient deceleration or acceleration of the heart rate, associated with premature ventricular contractions (*e.g.*, isolated, couplets and triplets) are frequently observed even from the first contact of the needle with the epicardium as well as during and/or shortly after IMI. However, no life-threatening arrhythmias are developed, and acute adverse effects are rarely observed using up to 0.25 mL (1.25×10^6 cells) of injectate per IMI injection site (see **Representative Results** and **Discussion**).

3.8. Perform subtle changes in the angle of incidence of the needle as necessary to complete injections of 0.25 mL to each of the four target IMI sites (three in the left ventricular free wall (LVFW) and one in the IVS).

3.9. After completing the percutaneous contrast echocardiography-guided IMI procedure, evaluate heart rhythm (*e.g.*, through serial ECG trace and/or 24 h Holter ECG), and perform serial window echocardiographic scans to verify the absence of complications, until the animal is fully recovered from anesthesia, and only then transfer to a light cycle room.

3.9.1. Here, we use 24 h Holter ECG to monitor the effects of IMI with InI on heart rhythm for 24 h. For this, we compared a group of 6 rabbits with normal phenotype (Normal Group) and a group of 6 rabbits that received intravenous administration of Doxorubicin (a cardiotoxic anthracycline drug, commonly used for the treatment of cancer; DOX group) at a dose of 2 mg/kg/week for 8 weeks, and then both cohorts received IMI with InI.

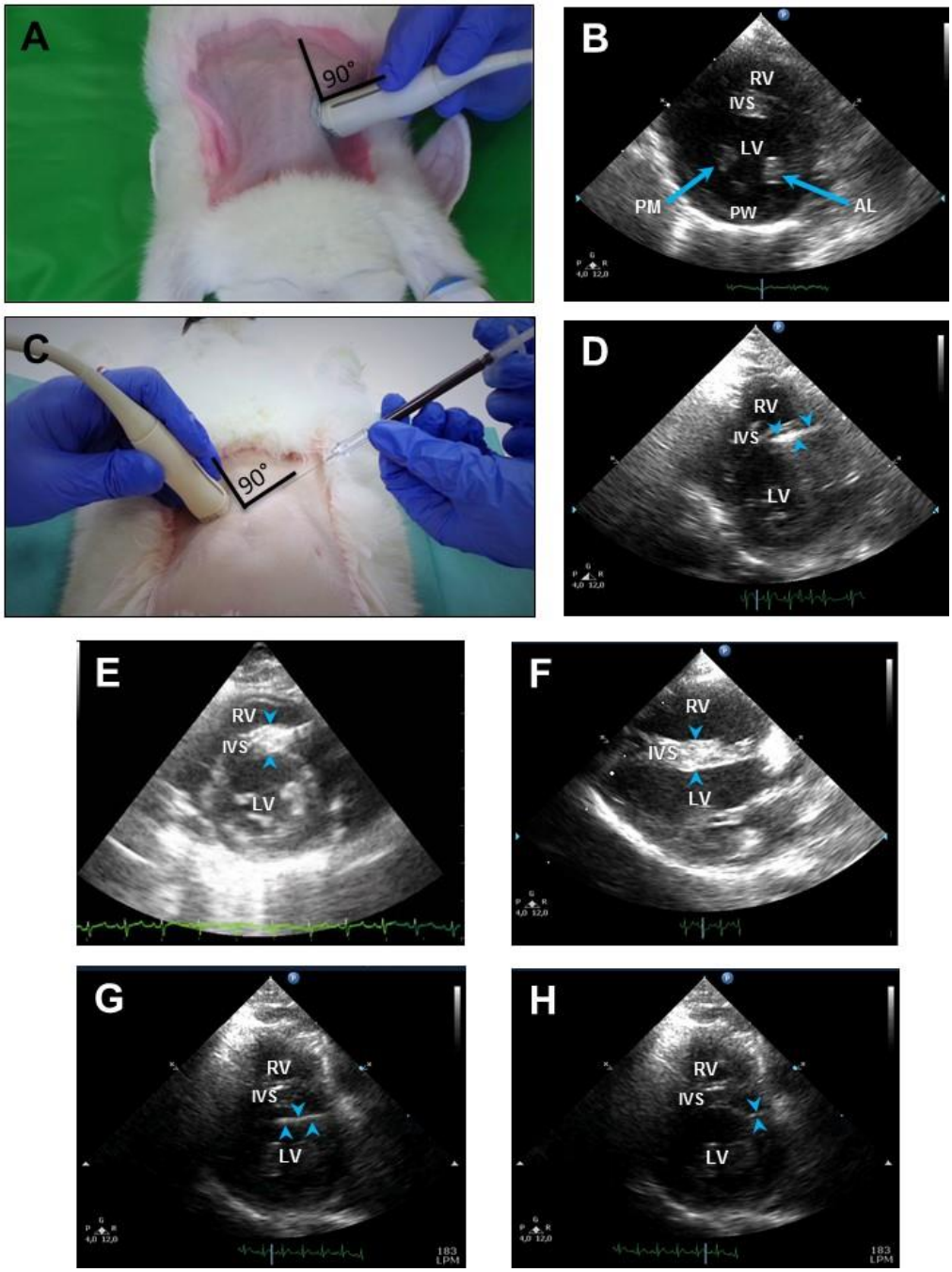

Figure 2. Percutaneous contrast echocardiography-guided intramyocardial injection in the rabbit. (**A**) Placement of the transducer in the right hemithorax at an angle of ~ 90°. (**B**) Representative image of a parasternal short axis view (PSSX) of the heart at the level of papillary muscles in the rabbit. (**C**) Alignment of the needle at an angle of ~ 90° relative to the transducer orientation mark. (**D**) Location of the needle at the target site in a PSSX view of the heart (note that the needle is easily visualized in the plane of the ultrasound beam). (**E** and **F**) Demonstration of hyperechogenicity at the target site upon intramyocardial injection with India Ink (arrowheads highlight the transmural hyperechogenicity). (**G**) Accidental location of the needle in the LV chamber (arrowheads highlight the needle shaft). (**H**) Repositioning of the needle to the LV free wall (arrowheads highlight the needle shaft). RV = right ventricle; LV = left ventricle; IVS = interventricular septum; PW = posterior wall; AL = anterolateral papillary muscle; PM = posteromedial papillary muscle.

4. Post IMI Analyses

4.1. Perform histopathological analysis of heart tissue samples from rabbits.

4.1.1. Fix tissue for 24 h in 10% formaldehyde, followed by dehydration with increasing ethanol concentrations as follows:

- 1x in 70% (60 min)
- 1x in 95% ethanol/5% methanol (60 min)
- 1x in 100% (60 min)
- 2x in 100% (90 min)
- 1x in 100% (120 min)

Note: All the above incubations are conducted at room temperature (RT). Then, substitute twice with 100% xylene (1 h, RT), and finally embed in paraffin in two steps (60 min, 58 °C)[25].

4.1.2. Perform 4–5 µm tissue sections with a microtome[25]. Mount sections on slides.

4.1.3. Perform staining with hematoxylin-eosin and Masson's trichrome methods[25-27].

4.2. In tissue sections from transplanted hearts, perform immunohistochemistry to detect EGFP(+) HEK-293 cells (*e.g.*, using the avidin-biotin complex (ABC) method), briefly:

4.2.1. De-wax 4–5 µm thick heart sections in 100% xylene (10 min, at RT). Rehydrate tissue by washing with decreasing ethanol concentration solutions (2x in 100% (2 min); 2x in 95% (2 min); 1x in 70% (2 min); 1x in 50% (2 min); 1x in 30% (2 min); 1x ddH_2O (2 min)) at RT.

4.2.2. Perform endogenous peroxidase inhibition by covering the sections with 100 µL of 3% H_2O_2 diluted in methanol (prepared with 5 mL of 30% stock solution of H_2O_2, and adding methanol up to a total volume of 50 mL) (incubate 30 min, RT), and then wash by immersion with Tris buffered saline (TBS; pH 7.6).

4.2.3. Perform antigen unmasking via enzymatic treatment, by covering the sections with 100 µL of 0.1% Pronase (prepared with 0.01 g Pronase diluted in 10 mL TBS) (incubate 12 min, RT), then wash with TBS (5 min, RT).

4.2.4. Incubate in blocking solution (normal goat serum at 10% in TBS) using 100 µL per slide (30 min, RT), and wash with TBS (5 min, RT).

4.2.5. Incubate with chicken anti-green florescent protein (GFP) as primary antibody (1:500 in TBS) (1 h, 30 °C), and wash with TBS (5 min, RT).

4.2.6. Incubate with secondary antibody biotinylated goat-anti-chicken IgG (1:250 in TBS) (1 h, 30 °C), and then wash with TBS (5 min, RT).

4.2.7. Incubate with avidin-biotin complex (20 min, 30 °C), and then label using 3,30-diaminobenzidine tetrahydrochloride (DAB) (RT, 5–10 min).

4.2.8. Finally, dehydrate by washing in increasing ethanol concentrations (1x in 30% (2 min); 1x in 50% (2 min); 1x in 70% (2 min); 2x in 95% (2 min); 2x in 100% (2 min)) at RT, counterstain sections using the hematoxylin-eosin method[25], and then mount cover slides. Include positive, negative as well as isotype controls.

Note: The brief protocol described above is not intended for general immunohistochemistry use; optimization for the tissue of interest and conditions is necessary.

REPRESENTATIVE RESULTS:

Percutaneous Contrast Echocardiography-guided IMI with InI:

Using the protocol described above, and once the optimal positioning of the tip of the needle was confirmed by echocardiography and the injection initiated, transmural hyperechogenicity was observed during the delivery of InI (10% v/v in PBS) (**Figure 2E**), as well as shortly after the IMI to the target region (**Figure 2F**). When IMI was immediately followed by euthanasia and the heart removed, deposits of InI were easily visible upon external examination of the heart (**Figure 3A**). In addition, heart tissue sections, *e.g.*, short axis section at the level of the papillary muscles (**Figure 3B**), revealed transmural deposits of InI dye at the injection site, thus demonstrating the successful and effective delivery of injectate into the myocardium using this technique. Of note, the transmural hyperechogenicity observed *in vivo* during IMI (**Figure 2E, F**), correlated well with transmural deposits of InI in *ex vivo* specimens (**Figure 3A, B**). This clearly demonstrated that InI has dual properties in the setting of IMI: as an *in vivo* ultrasound contrast agent, as well as an *ex vivo in situ* tracer. Both of these properties make InI a very versatile and inexpensive ultrasound contrast agent, particularly for training during the acquisition of competency in this technique. Thus, the echogenic properties of InI help to monitor IMI *e.g.*, determine successful IMI versus accidental intra-chamber or pericardial space injection, and, when necessary, given the real-time imaging capabilities of ultrasound, to make corrections of the needle track in real time (**Figure 2G, H**). On the other hand, the *in situ* tracing capabilities of InI are of value to locate the injectate in *ex vivo* specimens of the target myocardium.

Percutaneous Contrast Echocardiography-guided IMI with InI and EGFP(+) HEK-293 Cells:

Prior to IMI, successful transfection of EGFP(+) HEK-293 cells was confirmed by fluorescence microscopy during *in vitro* culture conditions (**Figure 3C**). The successful delivery of EGFP(+) HEK-293 cells into the myocardium was demonstrated via immunohistochemistry analysis of heart tissue sections where InI deposits were observed. Thus, using the avidin-biotin complex method (see step 4.2), abundant EGFP(+) HEK-293 cells were identified within the myocardium interspersed with InI deposits (**Figure 3D**). Deposits of InI were still observed 24 h after IMI in myocardial tissue samples from rabbits that received either InI in combination with EGFP(+) HEK-293 cells (**Figure 3E**), or InI alone (**Figure 3F**). Of note, an

acute inflammatory response was observed at this time point, with a predominant neutrophilic infiltrate, in samples from animals receiving EGFP(+) HEK-293 cells (**Figure 3E**), thus suggesting acute cellular rejection. On the other hand, macrophages were observed in animals receiving InI alone (**Figure 3F**).

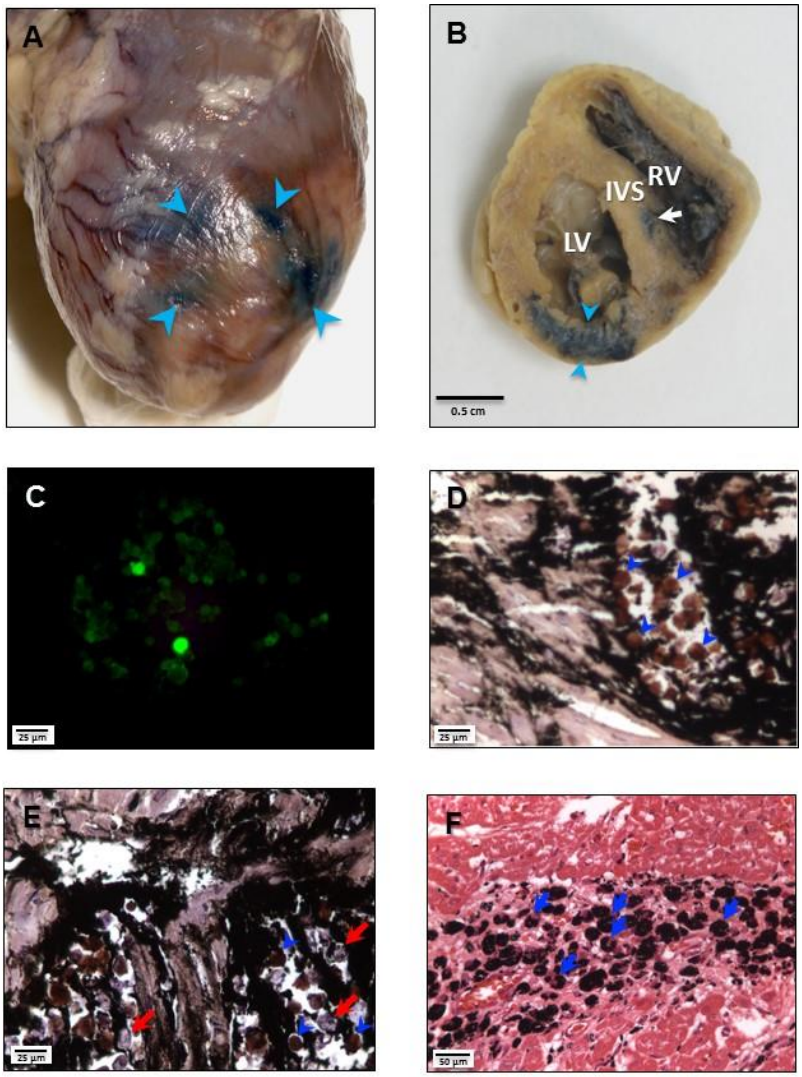

Figure 3. *In situ* macroscopic and histopathological evaluation and tracing of injectate. (**A**) Demonstration of the presence of injectate on external examination of an excised heart following IMI with InI (arrowheads highlight the sites of injection). (**B**) Demonstration of transmural distribution of injectate following IMI with InI in a transverse section of the heart at the level of the papillary muscles (blue arrowheads highlight the transmural InI deposit; white arrow highlights a visible deposit of InI at the IVS). (**C**) Autofluorescence *in vitro* of EGFP(+) HEK-293 cells using fluorescence microscopy. (**D–F**) Histopathological analysis of injected sites. EGFP(+) cells are visibly interspersed with InI deposits within the myocardium at 0 h (**D**) and 24 h (**E**) post IMI (blue arrowheads highlight EGFP(+) cells; red arrows highlight the presence of neutrophils). Deposits of InI interspersed within the myocardium at 24 h (**F**) following IMI with InI alone (blue arrows highlight the presence of macrophages). RV = right ventricle; LV = left ventricle; IVS = interventricular septum; IMI = Intramyocardial injection; InI = India Ink.

Having performed over 60 percutaneous contrast echocardiography-guided IMI procedures to date, we believe that with careful attention to detail and good animal handling and care, the procedure is generally well tolerated, and acute complications are very rare and usually mild. In general, in animals that undergo IMI, the most frequent observation during and shortly after the procedure is transient acceleration or deceleration of heart rate, associated with isolated premature ventricular complexes (PVC) (**Figure 4A**). Thus, 24 h Holter ECG monitoring of animals that received InI alone via IMI, revealed that the most frequent arrhythmia detected (total number of episodes within 24 h) was isolated PVC, even though a higher number of episodes were detected in animals that were previously treated with DOX for 8 weeks (**Figure 5A**). PVC in couplets and triplets appear to be less frequent (**Figure 4B, C** and **Figure 5B, C**), even though triplets are significantly less frequent in DOX-treated than in untreated Normal rabbits (**Figure 5C**). On the other hand, non-sustained ventricular tachycardia (NSVT) was more frequently observed in Normal animals (**Figure 4D** and **Figure 5D**). Significantly, whilst the mean heart rate was not different between DOX and Normal groups after receiving IMI with InI alone (**Figure 5E**), the standard deviation of normal R-R interval (SDNN), was significantly reduced (< 100 ms) in the DOX group (**Figure 5F**). The SDNN is a non-linear measure of heart health status, and therefore this result indicates that the DOX group has global alterations in its cardiac physiological status.

Figure 4. Ventricular arrhythmias observed during 24 h Holter monitoring in Rabbits that received IMI with InI. The images shown are screenshots obtained from Holter ECG tachograms displayed on screen during offline analysis, and illustrate representative examples of the most common types of arrhythmias found during 24 h of monitoring. (**A**) Isolated PVC. (**B**) PVC in Couplets. (**C**) PVC in Triplets. (**D**) NSVT. PVC = premature ventricular contractions; NSVT = non-sustained ventricular tachycardia.

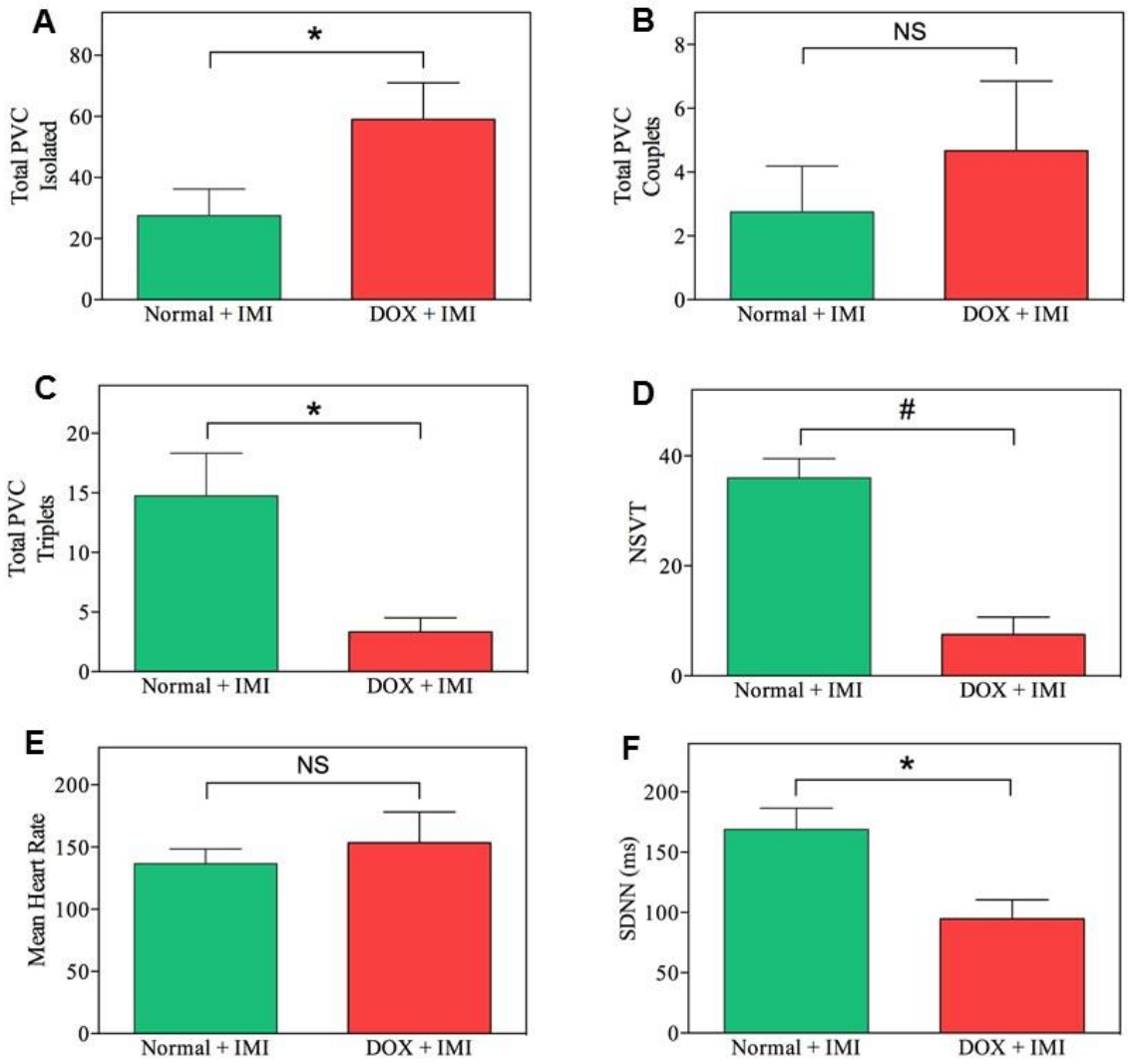

Figure 5. Arrhythmic events detected by 24 h Holter ECG monitoring following IMI with InI in rabbits. Total number of Isolated PVC (**A**), PVC in couplets (**B**), PVC in triplets, (**C**) and NSVT (**D**), in untreated rabbits (Normal + IMI) versus Doxorubicin-treated (3 mg/kg/week for 6 weeks) rabbits (DOX + IMI), after IMI with InI. Mean heart rate (**E**) and SDNN (**F**), in rabbits from Normal + IMI and DOX + IMI groups after IMI with InI. Data are expressed as mean ± SEM. * indicates $p < 0.05$; and # indicates $p < 0.01$, comparing Normal + IMI versus DOX + IMI groups by *t*-test.

DISCUSSION:

The primary goal was to develop a minimally-invasive technique that could be used for the delivery of stem cells into the myocardium of rabbits (a large sized preclinical animal model)[17,18], whilst taking advantage of the use of a relatively inexpensive imaging system readily available in many clinical and research centers. Here, we show that, using a clinical echocardiography system, and aided by InI, a widely available agent, with both *in situ* tracing capabilities and echogenic properties, successful percutaneous contrast echocardiography-guided IMI is very effective in delivering injectate to target regions of the rabbit heart. As far as we know, this is the first description of a percutaneous contrast

echocardiography-guided IMI and cell delivery in a large animal model such as the rabbit[18,19]. Whilst InI has been used previously in studies for *in situ* localization of injectate within tissues[7,28], this is to our knowledge, the first description of the dual properties of this agent as an *in vivo* ultrasound contrast agent and as an *in situ* tracer of injectate *ex vivo*. Indeed, complex mixtures of contrast agents and *in situ* tracing substances previously have been described in murine studies aimed at delivering injectates into the myocardium[29]. However, given the echogenic properties of InI and its *in situ* tracing capabilities, this substance could be very useful during competence acquisition whilst undergoing training with this technique.

Confirmation of delivery of injectate containing both InI as well as EGFP(+) HEK-293 cells using immunohistochemistry demonstrates the applicability of this technique to preclinical research aimed at stem cell therapy. An IMI of InI in conjunction with EGFP(+) HEK-293 resulted in an acute inflammatory response with a predominant neutrophilic infiltrate, suggesting a response of acute cellular rejection (within 24 h) to the xenogeneic cells. This response probably is not surprising in an immunocompetent animal. On the other hand, an IMI with InI alone also elicited an acute inflammatory response (within 24 h) in the treated myocardial tissue, which exhibited a predominant macrophage infiltrate. This is in line with the observation of acute inflammation described in previous studies following IMI under direct view in an open chest procedure[4,30-33]. Acute inflammation also has been observed upon injection of normal saline or PBS solutions into the myocardium[34,35], and even into the gastrocnemius muscles of the rat[36], and therefore this response has been attributed to direct tissue injury rather than to the injectate *per se*.[30-32,34-36] Indeed, the International Society for Cardiovascular Translational Research acknowledges the common occurrence of inflammation in the setting of IMI, but there is no consensus as to whether or not measures to reduce this process during the peri-procedural time are useful (*e.g.*, intravenous (I.V.) corticosteroids)[37]. Even though inflammation in this study could also be ascribed to direct tissue injury, the results also suggest that InI as a foreign body must also play a role in this process, provided a number of macrophages appear to be phagocytizing InI (**Figure 3F**). A thorough analysis of the functional effects of this acute inflammation secondary to IMI within the heart, or whether or not these can be ameliorated via administration of prophylactic drugs such as corticosteroids is beyond the scope of this manuscript. Nevertheless, percutaneous contrast echocardiography-guided IMI to four target regions of the myocardium, with a volume of injectate of up to 0.25 mL (1.25×10^6 cells) per IMI site, was very well tolerated in the rabbit.

With more than 60 procedures performed to date, and after competency was achieved, the mortality secondary to the procedure was very low. For example, no deaths occurred in the two cohorts described in step 3.9 (Normal and DOX groups) after IMI. Indeed, to date after 67 IMI procedures performed as part of an ongoing research program, we have only had two deaths directly related to the procedure (2.9% mortality). In one of these, the presence of a hemopericardium was demonstrated in the *post mortem* examination, whilst the other developed clinical neurological signs, consistent with acute cerebral ischemia secondary to a cardioembolic event, thus requiring a humane end-point. This mortality rate (2.9%) is significantly lower than that reported by Lu *et al.* (11%)[8] and Mu *et al. (*27%)[38], in rabbits that received IMI under direct view in an open chest procedure. Thus, we consider the procedure described in the current study to be safe, and we are using this technique in

ongoing studies to evaluate stem cell-based therapy in a rabbit model of AICM with promising results[39,40].

There are several critical points for a successful percutaneous contrast echocardiography-guided IMI. First, ensure that a parasternal short axis view at the level of the papillary muscles is obtained with clear delineation of the endocardial and epicardial contours. Next, ensure that the needle tip is within the field of view at all times once this has entered the chest cavity and the myocardium to prevent accidental delivery into the pericardial space or LV chamber. Then, make sure to keep to a minimum the number of passages through the chest cavity, and into the pericardium and myocardium, since this could increase the likelihood of local trauma (*e.g.*, laceration) to these structures, and the associated risk of hemopericardium. For this, whilst maintaining the needle in the chest cavity (and for some target sites, at the same point of entry in the visceral pericardium (*e.g.*, lateral wall)), carefully perform subtle changes in the angle of incidence of the needle. Finally, always use a needle that has a clear and easy passage through the skin into the chest cavity, thus avoiding blunt needle bevels from entering the myocardium and causing significant damage.

The procedure described herein, not only allows reliable and successful delivery of injectate to several target sites within the myocardium, but it also permits correction of the needle trajectory in real time, thus preventing accidental intrachamber delivery (**Figure 2G, H**). Whilst closed chest IMI procedures have been described previously in mice, there are several limitations inherent to this small animal model. These limitations include the number of target regions of the myocardium amenable to therapy, and the low volume/number of cells that can be injected per target site[29,41]. In addition, accurate delivery of the injectate is often a concern, with a success rate close to 60–70%[42], and therefore the use of less widely available high frequency ultrasound systems is usually required[29,41,42]. These systems are equipped with linear array transducers that also have inherent imaging limitations (*e.g.*, reverberation is a frequent artifact)[14]. Another limitation of small rodent models such as mice and rats, is their intrinsic differences in Ca^{+2} transport system and cellular electrophysiology, which differs from that of humans and large sized animal models such as dogs, pigs and rabbits[15,16,43]. All these limitations often create difficulties in translating the findings in these models into the clinic without prior confirmation in a large animal model.

Careful monitoring of the animal in the peri-procedural period is mandatory according to the contemporary guidelines for the care of laboratory animals. As shown here, this could be done by serial echocardiography window scans and ECG tracings, at least until the animal is awake from the anesthesia. The acute effects of IMI on heart rhythm also can be monitored by 24 h Holter ECG and is our standard practice. Of note, the most frequent arrhythmias were isolated PVC, which are relatively benign in nature, and which were more common in animals that have been treated with Doxorubicin prior to IMI with InI (see **Figure 4A** and **Figure 5A**). Other arrhythmias that were relatively less frequent include: PVC in couplets; PVC in triplets; as well as NSVT (see **Figure 4B–D** and **Figure 5B–D**). However, no life threatening arrhythmias such as sustained ventricular tachycardia were observed. Of note, we also found that some cardiotoxic manifestations in the DOX group could be detected by Holter ECG monitoring, using time frequency-domain variables of heart rate variability (HRV) such as SDNN. Thus, a reduced SDNN (**Figure 5E, F**), a non-linear measure

of heart health status, was observed in the DOX group compared to the Normal Group. This is the first report of reduced HRV, as demonstrated by a reduced SDNN, in the context of a rabbit model of AICM, which is in line with the observation that reduced SDNN is a powerful independent predictor of cardiac death in patients with HFrEF[44-46]. The alterations in SDNN in the DOX group are probably not related to the IMI procedure itself; nevertheless, confirmation of these findings in rabbits receiving Doxorubicin, as well as normal animals that do not receive IMI, is required. Whether reduced SDNN in HFrEF could also be improved, and therefore used as a surrogate measure of the benefit of stem cell based therapy, remains to be evaluated, and will be the focus of the future research.

Several routes of delivery of cells into the heart have been explored, including intravenous, intracoronary, and intramyocardial delivery; however, the intramyocardial route as used herein, has consistently shown the greatest level of cell retention rates[1-5,37]. We did not assess cell retention rate in the studies presented here, as the methodology used is not robust and specific enough to quantitate this *in vivo* or *ex vivo*, which is a limitation of this study. Instead, we used EGFP(+) HEK-293 cells whose phenotypic characteristics allowed us to easily discriminate the presence of these cells within the myocardium, thus indicating successful intramyocardial delivery. However, the main aim was to develop a minimally invasive technique whereby we could perform IMI and cell delivery into the myocardium of a large sized, preclinical model of non-ischemic cardiomyopathy. As demonstrated in **Figure 2** and **Figure 3**, this was accomplished for the first time by percutaneous contrast echocardiography-guided IMI. Further studies are necessary to assess cell retention rate as well as any potential beneficial effects of stem cells delivered into the myocardium using the procedure described herein; these studies are currently underway. We recently communicated promising results in regard to functional effects[39,40].

Compared to IMI in an open chest procedure, a percutaneous contrast echocardiography-guided IMI in a large preclinical model as described in this study, is significantly less invasive in nature with quick recovery of the animal following the procedure, and, as mentioned above, it also has lower mortality rate[8,38]. Another approach to IMI is catheter-based IMI, which also has been tested in preclinical models and several small clinical trials (for a review, see Sheng *et al.*)[47]. With this approach, a catheter is advanced into the LV cavity and then positioned at target sites within the endocardium. These target sites are either identified prior to the procedure, *e.g.*, using contrast cardiac magnetic resonance imaging (CMR)[48], or during the procedure, *e.g.*, by electromechanical endocardial mapping (EEM), to clearly differentiate viable myocardium prior to injection[49]. This latter approach is less invasive compared to open chest IMI under direct view, which is a clear advantage. Also, since IHD in humans has a patchy distribution, EEM helps direct the therapy specifically to viable sites of the myocardium, which is particularly important in the setting of IHD. However, a major drawback is the induction of ventricular arrhythmias, which are a common feature of all IMI approaches. Other drawbacks include the lengthy procedural time, providing EEM is a highly demanding technique which requires extensive training, and an associated risk of cardiac perforation. In contrast, percutaneous contrast echocardiography-guided IMI as described in this study, technically is less demanding than catheter-based IMI, and, once competency is achieved, it can be performed safely within 25 min after anesthesia. Similarly, since only a short portion of the needle is advanced into the

myocardium, there is a lower risk of cardiac perforation, though cardiac laceration is still possible.

In conclusion, the percutaneous contrast echocardiography-guided IMI technique described in this study in a large animal model, such as the rabbit[16,43], is safe, well tolerated, and effective in delivering the injectate into the heart. Therefore, it constitutes a promising strategy for preclinical hypothesis testing of the effects of cardiac regenerative therapeutics in non-ischemic cardiomyopathy (*e.g.*, AICM), including, but not limited to, stem cell-based therapy.

ACKNOWLEDGMENTS:
The authors thank Sheila Monfort, Brenda Martínez, Carlos Micó, Alberto Muñoz, and Manuel Molina for excellent support provided during the collection of data, and Carlos Bueno for providing the EGFP(+) HEK-293 cells. This work was supported in part by: Fundación Séneca, Agencia de Ciencia y Tecnología, Región de Murcia, Spain (JT) (Grant number: 11935/PI/09); Red de Terapia Celular, ISCIII-Sub. Gral. Redes, VI PN de I+D+I 2008-2011 (Grant no. RD12/0019/0001) (JMM), Co-financed with Structural funding of the European Union (FEDER) (JMM); and, the University of Reading, United Kingdom (AG, GB) (Central Funding). The funders had no role in study design, data collection and analysis, decision to publish, or preparation of the manuscript.

DISCLOSURES:
The authors have nothing to disclose.

REFERENCES:
1 Hou, D. *et al.* Radiolabeled cell distribution after intramyocardial, intracoronary, and interstitial retrograde coronary venous delivery: implications for current clinical trials. *Circulation* **112**, I150-156, doi:10.1161/CIRCULATIONAHA.104.526749 (2005).
2 Freyman, T. *et al.* A quantitative, randomized study evaluating three methods of mesenchymal stem cell delivery following myocardial infarction. *Eur Heart J* **27**, 1114-1122, doi:10.1093/eurheartj/ehi818 (2006).
3 Perin, E. C. *et al.* Comparison of intracoronary and transendocardial delivery of allogeneic mesenchymal cells in a canine model of acute myocardial infarction. *J Mol Cell Cardiol* **44**, 486-495, doi:10.1016/j.yjmcc.2007.09.012 (2008).
4 Dib, N., Khawaja, H., Varner, S., McCarthy, M. & Campbell, A. Cell therapy for cardiovascular disease: a comparison of methods of delivery. *J Cardiovasc Transl Res* **4**, 177-181, doi:10.1007/s12265-010-9253-z (2011).
5 Li, S. H. *et al.* Tracking cardiac engraftment and distribution of implanted bone marrow cells: Comparing intra-aortic, intravenous, and intramyocardial delivery. *J Thorac Cardiovasc Surg* **137**, 1225-1233 e1221, doi:10.1016/j.jtcvs.2008.11.001 (2009).
6 Shiba, Y. *et al.* Human ES-cell-derived cardiomyocytes electrically couple and suppress arrhythmias in injured hearts. *Nature* **489**, 322-325, doi:10.1038/nature11317 (2012).
7 Chong, J. J. *et al.* Human embryonic-stem-cell-derived cardiomyocytes regenerate non-human primate hearts. *Nature* **510**, 273-277, doi:10.1038/nature13233 (2014).
8 Lu, C. *et al.* Autologous bone marrow cell transplantation improves left ventricular function in rabbit hearts with cardiomyopathy via myocardial regeneration-unrelated mechanisms. *Heart vessels* **21**, 180-187, doi:10.1007/s00380-005-0886-9 (2006).

9 McMurray, J. J. *et al.* ESC guidelines for the diagnosis and treatment of acute and chronic heart failure 2012: The Task Force for the Diagnosis and Treatment of Acute and Chronic Heart Failure 2012 of the European Society of Cardiology. Developed in collaboration with the Heart Failure Association (HFA) of the ESC. *Eur J Heart Fail* **14**, 803-869, doi:10.1093/eurjhf/hfs105 (2012).
10 Sueta, C. A. The life cycle of the heart failure patient. *Curr Cardiol Rev* **11**, 2-3 (2015).
11 Carver, J. R. *et al.* American Society of Clinical Oncology clinical evidence review on the ongoing care of adult cancer survivors: cardiac and pulmonary late effects. *J Clin Oncol* **25**, 3991-4008, doi:JCO.2007.10.9777 [pii]
10.1200/JCO.2007.10.9777 (2007).
12 Verdecchia, A. *et al.* Recent cancer survival in Europe: a 2000-02 period analysis of EUROCARE-4 data. *Lancet Oncol* **8**, 784-796, doi:S1470-2045(07)70246-2 [pii]
10.1016/S1470-2045(07)70246-2 (2007).
13 De Angelis, R. *et al.* Cancer survival in Europe 1999-2007 by country and age: results of EUROCARE--5-a population-based study. *Lancet Oncol* **15**, 23-34, doi:10.1016/S1470-2045(13)70546-1 (2014).
14 Abu-Zidan, F. M., Hefny, A. F. & Corr, P. Clinical ultrasound physics. *J Emerg Trauma Shock* **4**, 501-503, doi:10.4103/0974-2700.86646 (2011).
15 Del, M. F., Mynett, J. R., Sugden, P. H., Poole-Wilson, P. A. & Harding, S. E. Subcellular mechanism of the species difference in the contractile response of ventricular myocytes to endothelin-1. *Cardioscience* **4**, 185-191 (1993).
16 Pogwizd, S. M. & Bers, D. M. Rabbit models of heart disease. *Drug Discov Today Dis Mod* **5**, 185-193, doi:http://dx.doi.org/10.1016/j.ddmod.2009.02.001 (2008).
17 Gandolfi, F. *et al.* Large animal models for cardiac stem cell therapies. *Theriogenology* **75**, 1416-1425, doi:10.1016/j.theriogenology.2011.01.026 (2011).
18 Harding, J., Roberts, R. M. & Mirochnitchenko, O. Large animal models for stem cell therapy. *Stem Cell Res Ther* **4**, 23, doi:10.1186/scrt171 (2013).
19 Chong, J. J. & Murry, C. E. Cardiac regeneration using pluripotent stem cells--progression to large animal models. *Stem Cell Res* **13**, 654-665, doi:10.1016/j.scr.2014.06.005 (2014).
20 Talavera, J. *et al.* An Upgrade on the Rabbit Model of Anthracycline-Induced Cardiomyopathy: Shorter Protocol, Reduced Mortality, and Higher Incidence of Overt Dilated Cardiomyopathy. *BioMed Res Int* **2015**, 465342, doi:10.1155/2015/465342 (2015).
21 Bueno, C. *et al.* Human adult periodontal ligament-derived cells integrate and differentiate after implantation into the adult mammalian brain. *Cell Transplant* **22**, 2017-2028, doi:10.3727/096368912X657305 (2013).
22 Sahn, D. J., DeMaria, A., Kisslo, J. & Weyman, A. Recommendations regarding quantitation in M-mode echocardiography: results of a survey of echocardiographic measurements. *Circulation* **58**, 1072-1083 (1978).
23 Thomas, W. P. *et al.* Recommendations for standards in transthoracic two-dimensional echocardiography in the dog and cat. Echocardiography Committee of the Specialty of Cardiology, American College of Veterinary Internal Medicine. *J Vet Intern Med* **7**, 247-252 (1993).
24 Lang, R. M. *et al.* Recommendations for cardiac chamber quantification by echocardiography in adults: an update from the American Society of

Echocardiography and the European Association of Cardiovascular Imaging. *Eur Heart J Cardiovasc Imaging* **16**, 233-270, doi:10.1093/ehjci/jev014 (2015).

25 Feldman, A. T. & Wolfe, D. Tissue processing and hematoxylin and eosin staining. *Methods Mol Biol* **1180**, 31-43, doi:10.1007/978-1-4939-1050-2_3 (2014).

26 Howat, W. J. & Wilson, B. A. Tissue fixation and the effect of molecular fixatives on downstream staining procedures. *Methods* **70**, 12-19, doi:10.1016/j.ymeth.2014.01.022 (2014).

27 Cohen, A. H. Masson's trichrome stain in the evaluation of renal biopsies. An appraisal. *Am J Clin Pathol* **65**, 631-643 (1976).

28 Corti, R. *et al.* Real time magnetic resonance guided endomyocardial local delivery. *Heart* **91**, 348-353, doi:10.1136/hrt.2004.034363 (2005).

29 Springer, M. L. *et al.* Closed-chest cell injections into mouse myocardium guided by high-resolution echocardiography. *Am J Physiol Heart Circ Physiol* **289**, H1307-1314, doi:10.1152/ajpheart.00164.2005 (2005).

30 Aoki, M. *et al.* Efficient in vivo gene transfer into the heart in the rat myocardial infarction model using the HVJ (Hemagglutinating Virus of Japan)--liposome method. *J Mol Cell Cardiol* **29**, 949-959, doi:10.1006/jmcc.1996.0337 (1997).

31 Guzman, R. J., Lemarchand, P., Crystal, R. G., Epstein, S. E. & Finkel, T. Efficient gene transfer into myocardium by direct injection of adenovirus vectors. *Circ Res* **73**, 1202-1207 (1993).

32 Magovern, C. J. *et al.* Direct in vivo gene transfer to canine myocardium using a replication-deficient adenovirus vector. *Ann Thorac Surg* **62**, 425-433; discussion 433-424 (1996).

33 Suzuki, K. *et al.* Role of interleukin-1beta in acute inflammation and graft death after cell transplantation to the heart. *Circulation* **110**, II219-224, doi:10.1161/01.CIR.0000138388.55416.06 (2004).

34 Fukushima, S. *et al.* Direct intramyocardial but not intracoronary injection of bone marrow cells induces ventricular arrhythmias in a rat chronic ischemic heart failure model. *Circulation* **115**, 2254-2261, doi:10.1161/CIRCULATIONAHA.106.662577 (2007).

35 Vela, D. & Maximilian Buja, L. in *Stem Cell and Gene Therapy for Cardiovascular Disease* eds Leslie W. Miller, Doris A. Taylor, & James T. Willerson) 13-23 (Academic Press, 2016).

36 Fargas, A., Roma, J., Gratacos, M. & Roig, M. Distribution and effects of a single intramuscular injection of India ink in mice. *Ann Anat* **185**, 183-187, doi:10.1016/S0940-9602(03)80086-9 (2003).

37 Dib, N. *et al.* Recommendations for successful training on methods of delivery of biologics for cardiac regeneration: a report of the International Society for Cardiovascular Translational Research. *JACC Cardiovasc Interv* **3**, 265-275, doi:10.1016/j.jcin.2009.12.013 (2010).

38 Mu, Y., Cao, G., Zeng, Q. & Li, Y. Transplantation of induced bone marrow mesenchymal stem cells improves the cardiac function of rabbits with dilated cardiomyopathy via upregulation of vascular endothelial growth factor and its receptors. *Exp Biol Med (Maywood)* **236**, 1100-1107, doi:10.1258/ebm.2011.011066 (2011).

39 Giraldo, A. *et al.* Percutaneous intramyocardial injection of amniotic membrane-derived mesenchymal stem cells improves ventricular function and survival in non-ischaemic cardiomyopathy in rabbits. *Eur Heart J* **36**, 149 (2015).
40 Giraldo, A. *et al.* Allogeneic amniotic membrane-derived mesenchymal stem cell therapy is cardioprotective, restores myocardial function, and improves survival in a model of anthracycline-induced cardiomyopathy. *Eur J Heart Fail* **19**, 594, doi:DOI: 10.1002/ejhf.833 (2017).
41 Prendiville, T. W. *et al.* Ultrasound-guided transthoracic intramyocardial injection in mice. *J Vis Exp* e51566, doi:10.3791/51566 (2014).
42 Laakmann, S. *et al.* Minimally invasive closed-chest ultrasound-guided substance delivery into the pericardial space in mice. *Naunyn Schmiedebergs Arch Pharmacol* **386**, 227-238, doi:10.1007/s00210-012-0815-2 (2013).
43 Hasenfuss, G. Animal models of human cardiovascular disease, heart failure and hypertrophy. *Cardiovasc Res* **39**, 60-76 (1998).
44 Ponikowski, P. *et al.* Depressed heart rate variability as an independent predictor of death in chronic congestive heart failure secondary to ischemic or idiopathic dilated cardiomyopathy. *Am J Cardiol* **79**, 1645-1650 (1997).
45 Nolan, J. *et al.* Prospective study of heart rate variability and mortality in chronic heart failure: results of the United Kingdom heart failure evaluation and assessment of risk trial (UK-heart). *Circulation* **98**, 1510-1516 (1998).
46 Galinier, M. *et al.* Depressed low frequency power of heart rate variability as an independent predictor of sudden death in chronic heart failure. *Eur Heart J* **21**, 475-482, doi:10.1053/euhj.1999.1875 (2000).
47 Sheng, C. C., Zhou, L. & Hao, J. Current stem cell delivery methods for myocardial repair. *BioMed Res Int* **2013**, 547902, doi:10.1155/2013/547902 (2013).
48 Kim, R. J. *et al.* The use of contrast-enhanced magnetic resonance imaging to identify reversible myocardial dysfunction. *N Engl J Med* **343**, 1445-1453, doi:10.1056/NEJM200011163432003 (2000).
49 Perin, E. C. *et al.* Transendocardial, autologous bone marrow cell transplantation for severe, chronic ischemic heart failure. *Circulation* **107**, 2294-2302, doi:10.1161/01.CIR.0000070596.30552.8B (2003).